Available online at www.sciencedirect.com
SCIENCE DIRECT
Journal of Catalysis 229 (2005) 332–343
JOURNAL OF CATALYSIS
www.elsevier.com/locate/jcat

Pd-PVP colloid as catalyst for Heck and carbonylation reactions: TEM and XPS studies

Andrzej Gniewek [a], Anna M. Trzeciak [a,*], Józef J. Ziółkowski [a], Leszek Kępiński [b], Józef Wrzyszcz [b], Włodzimierz Tylus [c],

[a] *Faculty of Chemistry, University of Wrocław, 14 F. Joliot-Curie, 50-383 Wrocław, Poland*
[b] *Institute of Low Temperature and Structure Research Polish Academy of Sciences, PO Box 937, 50-950 Wrocław, Poland*
[c] *Wrocław University of Technology, Institute of Inorganic Technology, 27 Wybrzeże Wyspiańskiego, 50-370 Wrocław, Poland*

Received 13 September 2004; revised 28 October 2004; accepted 1 November 2004

Available online 24 December 2004

Abstract

Pd-PVP colloid (stabilized with polyvinylpyrrolidone) with a diameter of 19.8 nm in $[Bu_4N]Br$ medium catalyzes Heck coupling of bromobenzene with butyl acrylate and methoxycarbonylation of iodobenzene reactions. Oxidative addition of PhI or PhBr to Pd-PVP as the first step of a catalytic reaction was confirmed by TEM and XPS measurements. TEM studies showed significant reduction of Pd nanoparticle size after their reaction with PhX (X = I, Br) and $[Bu_4N]X$ (X = Cl, Br, I). The biggest shift of the center of nanoparticle size distribution, from 19.8 nm to 7.6 nm, was found when Pd-PVP reacted with PhI and $[Bu_4N]Br$. The formation of $[Bu_4N]_2[Pd(Ph)Br_3]$- and $[Bu_4N]_2[PdBr_4]$-type complexes in that system was evidenced by XPS and UV–vis spectra.

Keywords: Pd-PVP colloid; Heck reaction; Methoxycarbonylation; XPS; TEM; Redispersion of Pd

1. Introduction

The extraordinary catalytic properties of palladium in C–C bond formation reactions are well documented in the literature [1,2]. Among such reactions, a special place is occupied by palladium-catalyzed reactions with aryl halides as the substrates. Depending on the reaction conditions, aryl halides can be transformed into carboxylic acids, esters, or amides in a one-stage carbonylation process [1]. Olefination of aryl halides, the so-called Heck reaction, produces functionalized olefins and may be used for the synthesis of multifunctional derivatives [1,3], including natural products [4] and pharmaceuticals [5]. The Suzuki reaction produces biphenyl derivatives [6], and in the Sonogashira process phenylated alkines are obtained [7].

Palladium compounds, usually complexes with phosphane ligands, are very often used as catalyst precursors in the above-mentioned reactions. Phosphanes play the role of stabilizers of in situ formed soluble Pd(0) complexes, which are generally considered the catalytically active forms [8]. On the other hand, phosphane-free catalysts have recently generated great interest as a less complicated, environmentally friendly, and cheaper alternative to phosphane-containing systems [9–11]. However, the major disadvantage of phosphane-free catalysts is their low stability due to the formation of usually catalytically inactive "palladium black."

Recently, palladium nanoparticles have often been considered to be responsible for the activity of phosphane-free catalytic systems, as confirmed by experiments in some cases [12–14]. Reetz has shown that under Heck reaction conditions the $PdCl_2(PhCN)_2$ complex is transformed into palladium(0) nanoparticles [12]. The formation of Pd(0) nanoparticles under the sonochemical reaction has been es-

* Corresponding author.
E-mail address: ania@wchuwr.chem.uni.wroc.pl (A.M. Trzeciak).

0021-9517/$ – see front matter
doi:10.1016/j.jcat.2004.11.003

tablished by in situ TEM analyses [13]. It has also been proved that palladium nanoparticles are formed during reduction of the $PdCl_2$(cod) complex under carbonylation reaction conditions [14].

Their high surface-to-volume ratios make metal colloids very good candidates for active catalysts, but their thermodynamic instability complicates practical applications [15]. The first experiments with palladium colloid as catalyst in the Heck reaction of unactivated aryl bromides gave a low yield of products [16,17]. Yields of only up to 20% of ester were obtained in carbonylation of benzyl bromide catalyzed by $PdCl_2$(cod) and in carbonylation of iodobenzene with Pd colloid stabilized with *N*-polyvinylpyrrolidone (PVP) [14]. Very recently it was demonstrated that the Heck reaction goes smoothly at very low concentrations of palladium nanoparticles [18].

One of the most effective ways to increase the Heck reaction yield was to apply so-called Jeffery conditions, that is, the introduction of tetraalkylammonium salts to the reaction medium [19–21]. The use of ammonium salts has made it possible to obtain very good results in a number of Heck reactions [22–24] and carbonylation and Suzuki reactions [25,26]. However, the role of ammonium salts and their interactions with palladium catalyst have not been examined in detail, and usually ammonium salts are regarded as stabilizers of metal colloids, preventing their aggregation [27–29].

In this paper we present results demonstrating a very important function of ammonium salts in the solubilization of active palladium species formed in the reaction of Pd colloid with aryl halide. Similar interactions have been postulated by Reetz but have not been fully proved experimentally. Our studies were performed with a model system containing specially prepared Pd(0) colloid (with PVP as a protecting agent) of relatively large nanoparticles (19.8 nm diameter). We studied the interactions of Pd(0) species with particular components of the catalytic system, PhBr or PhI, $[Bu_4N]Br$, and $CH_2{=}CHC(O)OBu$, with XPS and TEM techniques.

2. Experimental

2.1. Reactants

Methanol, Et_3N, and diethyl ether were purified by standard procedures [30]. Iodobenzene and mesitylene (POCh, Gliwice, Poland) were used without purification. Ammonium salts ($[Bu_4N]X$, X = Cl, Br, I) were purchased from Fluka, and PVP K-30 (*N*-polyvinylpyrrolidone, M_w = 40,000) was purchased from Fluka and used without purification.

2.2. Synthesis of Pd-PVP catalyst

Three grams of PVP with an average molecular mass of 40,000 Da was added to 65 cm^3 of water and intensively stirred until the polymer was totally dissolved. Next, 5 cm^3 of an acidic (HCl) solution of $PdCl_2$, containing 0.03 g Pd in 1 cm^3, was added and warmed to 85 °C. When the temperature of the solution was stabilized, 0.4 g of pyrogallol dissolved in 20 cm^3 of water was added and stirred for 20 min and then cooled to the ambient temperature. The dark-brown colloidal suspension obtained was dried in a desiccator over molecular sieves (13X). The product obtained was a dark-brown lamellar Pd-PVP colloid containing 5% Pd. An X-ray powder diffractogram (Fig. 1) was obtained with a DRON-3 powder diffractometer equipped with a Cu-K_α line. According to the Scherrer equation, the mean diameter of Pd nanoparticles related to the width of the diffracted beam at $2\Theta = 40.1°$ was estimated to be 19.8 nm.

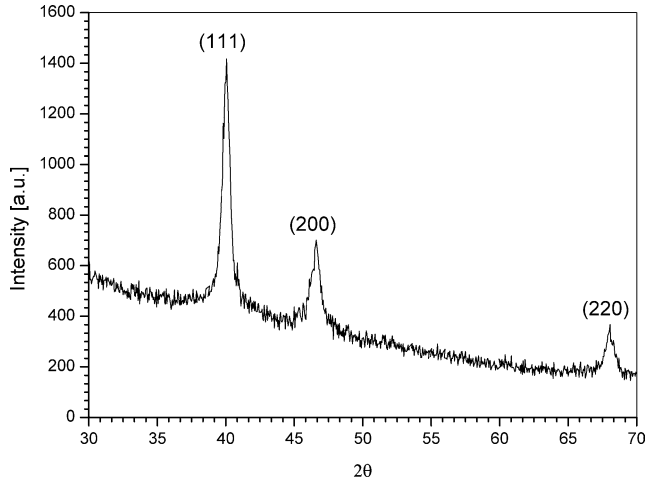

Fig. 1. XRD diffractogram of Pd nanoparticles in Pd-PVP colloid.

2.3. TEM studies

Transmission electron microscopy (TEM) was performed with a Philips CM-20 Super Twin microscope operating at 200 kV, providing a resolution of 0.25 nm.

2.4. Sample preparation for TEM and XPS studies

Seventy-five milligrams of Pd-PVP colloid was dissolved in methanol (1 cm^3), and then the remaining components, such as iodobenzene (or bromobenzene) and *n*-tetrabutylammonium salt in the molar ratio described in Table 4, were added. The solution obtained was refluxed at 140 °C for 4 h. Next, the solution was left in an open vessel until total removal of volatiles and dried in vacuo. The samples obtained were used for XPS measurements. The samples for TEM measurements were weighted in equal portions, each containing 5 mg of palladium. Each such portion was dissolved in 10 cm^3 of spectral-purity methanol. One drop of the solution was placed on the carbon-coated grid and dried for 40 min. The nanoparticle size distribution for each sample was determined by counting the size of approximately 300 palladium nanoparticles from several TEM images obtained from different places on the TEM grids. The size distribution

plots were fitted with the use of a Gauss curve approximation and the Microcal Origin program. The full width at half-maximum (FWHM) of the distribution makes it possible to estimate the breadth of the size distribution of nanoparticles, and the position of the center of the distribution indicates the most probable size of the nanoparticles.

2.5. XPS measurements

XPS spectra were recorded on a SPECS UHV/XPS/AES system equipped with a dual Mg/Al X-ray source and a hemispherical PHOIBOS 100 analyzer operating in the fixed analyzer transmission (FAT) mode. High-resolution spectra were obtained with a pass energy of 8 or 10 eV; a Mg-K_α X-ray source was operated at 250 W and 10 kV. The working pressure in the analyzing chamber was less than 5×10^{-10} mbar. The spectrometer energy scale was calibrated with Au $4f_{7/2}$, Ag $3d_{5/2}$, and Cu $2p_{3/2}$ lines at 84.2, 367.9, and 932.4 eV, respectively. Correction of the energy shift due to the static charging of the samples was accomplished with the C 1*s* peak at 284.6 eV as a reference. The accuracy of the reported binding energies was ±0.1 eV. For the XPS analysis, we obtained all sample specimens by pressing sample powders into thin disks, which were mounted on sample holders and placed in a prechamber, outgassed to less than 10^{-8} mbar at room temperature, and then transferred to the analysis chamber. Stability of Pd spectra during the XPS measurements was proved by a series of successive measurements. The spectra were collected and processed by SpecsLab software. The data analysis procedure involved data smoothing and background calculation with the Voight function, which is a convolution of Gaussian instrumental function and Lorentzian function for the natural line shape.

2.6. Catalytic reactions

2.6.1. Carbonylation reaction

The reactions were carried out in a 130 cm^3 thermostated steel autoclave with magnetic stirring. Reagents [PhI 1.1 cm^3 (9.5×10^{-3} mol), NEt_3 3.0 cm^3 (2.15×10^{-2} mol), mesitylene–internal standard, 0.64 cm^3 (4.6×10^{-3} mol), methanol 1.0 cm^3, Pd-PVP 0.032 g (1.5×10^{-5} mol), and $[Bu_4N]Br$ 3.22 g (1×10^{-2} mol)] were introduced to the autoclave in a N_2 atmosphere. Next, the N_2 atmosphere was replaced with CO. The reactions were carried out at 90 °C for 3 h. Afterward, the autoclave was cooled down and organic products were separated by extraction with diethyl ether (three times with 3 cm^3) and analyzed by GC-MS (Hewlett Packard 8452A). The solid residue was dried and used in the next reaction.

2.6.2. Heck reaction

The reactions were carried out in a 50 cm^3 Schlenk tube with magnetic stirring. Reagents [PhBr 0.24 cm^3 (2.3×10^{-3} mol) or 0.48 cm^3 (4.6×10^{-3} mol), CH_2=CHC(O)OBu 0.27 cm^3 (1.9×10^{-3} mol), $[Bu_4N]Br$ 0.75 g (2.3×10^{-3} mol), $NaHCO_3$ 0.4 g (4.8×10^{-3} mol) and Pd-PVP 0.030 g (1.5×10^{-5} mol)] were introduced to the Schlenk tube under a N_2 atmosphere. The reaction was carried out at 130–150 °C for 2–6 h. Afterward, organic products were separated by extraction with diethyl ether (three times with 5 cm^3) and analyzed by GC-MS (Hewlett Packard 8452A).

3. Results and discussion

3.1. Catalytic activity of Pd-PVP colloid

The catalytic activity of Pd-PVP colloid was first tested in the Heck reaction of bromobenzene with butyl acrylate (Scheme 1). In reaction with only Pd-PVP colloid after 4 h, 28% of the monoarylated product was obtained, and only 30% was obtained after 6 h (Table 1). A significant increase in bromobenzene and acrylate conversions and the yield of the products (mono- and diarylated) were observed when $[Bu_4N]Br$ was added to the reaction medium (Scheme 1, Table 1).

The tendency to form diarylated products is very distinct and was observed even when the reactant ratio ([PhBr]/[acrylate]) was 1.2 (Table 1). In reactions carried out with an excess of PhBr ([PhBr]/[acrylate] = 2.3), first (after 2 h) the monoarylated product dominated, but after 4 h the [monoaryl]/[diaryl] ratio was 26/73. A very significant temperature effect was noted: a temperature increase from 140 to 150 °C increased the rate of diarylated product formation to a yield of 93–94% after 2 h.

To investigate the possibility of catalyst recycling, the organic products of the reaction were carefully extracted

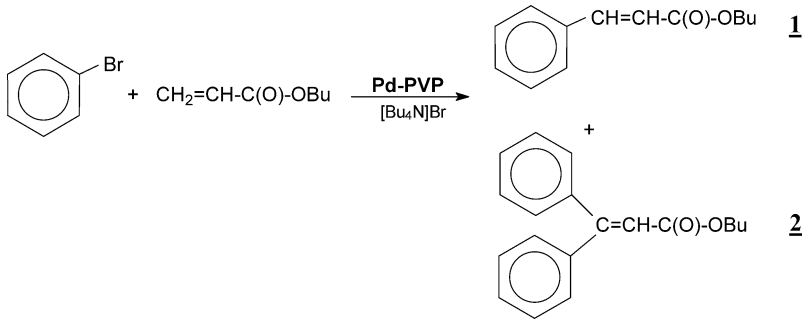

Scheme 1.

Table 1
Results of Heck reaction of PhBr with butyl acrylate (acr) catalyzed by Pd-PVP in $[Bu_4N]Br$

[acr]/[Pd]	Temp. (°C)	Time (h)	Yield of products (%)	
			Monoarylated (**1**)	Diarylated (**2**)
136[a]	130	4	28	–
		6	30	
172	130	2	73	–
		4	35	63
		6	20	77
136[b]	130	4	64	26
136[c]	130	4	73	27
136	130	2	75	8
		4	26	73
136	140	2	4	93
		4	1	95
136	150	2	1	94
		4	1	96

Reaction conditions: PhBr, 0.24 cm^3 (2.3×10^{-3} mol) or 0.48 cm^3 (4.6×10^{-3} mol); $CH_2{=}CHC(O)OBu$, 0.27 cm^3 (1.9×10^{-3} mol); $[Bu_4N]Br$, 0.75 g (2.3×10^{-3} mol); $NaHCO_3$, 0.4 g (4.8×10^{-3} mol), or HCOONa 0.324 g (4.8×10^{-3} mol); and Pd-PVP, 0.015 or 0.030 g.
[a] Reaction without $[Bu_4N]Br$.
[b] [PhBr]/[acr] = 1.2, base: $NaHCO_3$.
[c] [PhBr]/[acr] = 2.3, base: HCOONa.

Table 2
Results of Heck reaction of PhBr with butyl acrylate (acr) catalyzed by Pd-PVP in $[Bu_4N]Br$ with catalyst recycling

[acr]/[Pd]	Temp. (°C)	Time (h)	Yield of products (%)	
			Monoarylated (**1**)	Diarylated (**2**)
136[a]	130	4	26	74
		4	79	19
		4	72	1
		4	18	–
172[a]	130	4	35	65
		4	68	–
		4	57	–
		4	11	–
136[b]	140	2	41	57
		4	31	66
		4	54	46
		4	–	–
136[c]	140	2	17	78
		4	47	49
		4	66	28
		4	87	2

Reaction conditions: PhBr, 0.24 cm^3 (2.3×10^{-3} mol) or 0.48 cm^3 (4.6×10^{-3} mol); $CH_2{=}CHC(O)OBu$, 0.27 cm^3 (1.9×10^{-3} mol); $[Bu_4N]Br$, 0.75 g (2.3×10^{-3} mol); $NaHCO_3$, 0.4 g (4.8×10^{-3} mol); and Pd-PVP, 0.015 or 0.03 g.
Base: [a] $NaHCO_3$; [b] $NaHCO_3 + NEt_3$, 0.03 cm^3 (2.15×10^{-4} mol); [c] HCOONa, 0.0324 g (4.8×10^{-3} mol).

Table 3
Results of methoxycarbonylation reaction of PhI (yield of methyl benzoate, mol%) catalyzed by Pd-PVP or $[Bu_4N]_2[PdBr_4]$ in $[Bu_4N]Br$ with catalyst recycling

Catalyst	Run 1 (2 h)	Run 2 (2 h)	Run 3 (2 h)	Run 4 (2 h)
Pd-PVP	72	35	14	5
$[Bu_4N]_2[PdBr_4]$	100	74	53	33

Reaction conditions: PhI, 1.1 cm^3 (9.5×10^{-3} mol); $[Bu_4N]Br$, 3.22 g (1×10^{-2} mol); NEt_3, 3.0 cm^3 (2.15×10^{-2} mol); Pd-PVP, 0.032 g (1.5×10^{-5} mol) or $[Bu_4N]_2[PdBr_4]$, 0.0138 g (1.5×10^{-5} mol); 2 h, 5 atm CO, 90 °C.

with diethyl ether, and the remaining Pd catalyst dissolved in ammonium salt was reused. In successive catalytic reaction cycles carried out at 130 °C with $NaHCO_3$ added as a base, we observed (after 4 h) a significant decrease in diarylated product yield, and in the third cycle the monoarylated product was practically the only one formed (Table 2). More of the diarylated product was obtained when triethylamine (NEt_3) or sodium formate (HCOONa) was used as the base. The system with sodium formate in particular was found not only to be very active but also relatively stable, as demonstrated by the high yield of the reaction products, and even in the fourth cycle 89% mono- and diarylated products were obtained (Table 3). The results obtained demonstrate quite good efficiency of Pd-PVP as a catalyst in the Heck reaction of nonactivated bromobenzene in the presence of ammonium salt as a component of the catalytic system. The gradual decrease in the activity of the recovered Pd-PVP catalyst is partially explained by the negative side effect of accumulated NaBr, whose concentration increases over the reaction time. The oxidation of Pd(0) to Pd(II) during catalyst recovery can also negatively influence the reaction course.

Pd-PVP is also active in methoxycarbonylation of iodobenzene in methanol with the addition of $[Bu_4N]Br$ (Scheme 2). Methyl benzoate with 100% yield was obtained in 3 h at 90 °C. As in the case of the Heck reaction, the addition of $[Bu_4N]Br$ improved the activity of Pd-PVP colloid (up to 100% yield) compared with only a 20% yield of methyl benzoate under identical reaction conditions, but in the absence of ammonium salt.

A comparison of catalytic activity of Pd-PVP colloid and $[Bu_4N]_2[PdBr_4]$ complex in methoxycarbonylation of iodobenzene is presented in Table 3. The slightly higher yields obtained with $[Bu_4N]_2[PdBr_4]$ complex may be explained by its better solubility in reaction medium.

3.2. TEM studies of Pd-PVP in Heck reaction conditions

The results of TEM studies of the Pd-PVP colloid samples as prepared made it possible to conclude that palla-

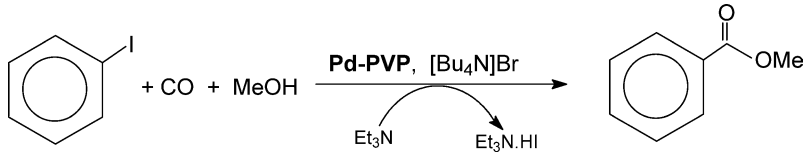

Scheme 2.

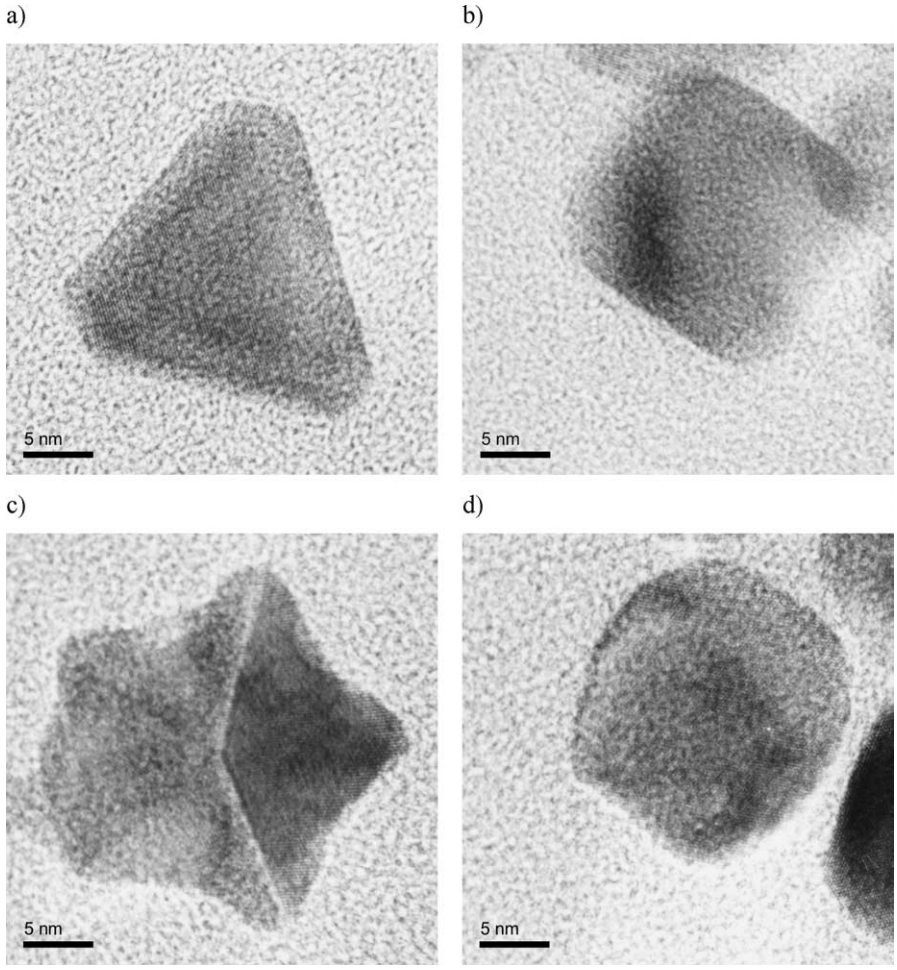

Fig. 2. TEM micrographs showing typical shapes of Pd nanoparticles in the as prepared Pd-PVP colloid: triangular (a), rhombohedral (b), pentagonal (c), and unidentified shape (d).

dium nanoparticles have mostly very well-defined geometrical shapes. One may distinguish the following shapes of nanoparticles: triangle, rhomboidal or square, and pentagonal (Figs. 2a–c). Relatively few particles had less defined shapes (Fig. 2d). This observation is in agreement with similar studies described in the literature [31,32]. The size distribution of as-prepared Pd-PVP nanoparticles is shown in Fig. 3a. The histogram could be fitted to a Gaussian function, yielding a maximum at 19.8 nm and a FWHM of 7.0 nm.

TEM results for Pd-PVP colloid isolated after the reaction with particular components of the catalytic system made it possible to monitor interactions of the nanoparticles with the reactants under Heck reaction conditions [33]. Pd-PVP sample heated with only $[Bu_4N]Br$ (Fig. 3b) demonstrated that the Pd nanoparticle size distribution is practically the same as for the Pd colloid as prepared (Fig. 3a), with the center of size distribution at 19.8 nm (Table 4).

Quite different results were obtained when the Pd-PVP colloid was warmed with aryl halides like iodobenzene (PhI) or bromobenzene (PhBr). The results of interactions are seen both on the TEM images and on the histograms presenting the nanoparticle size distribution. Reaction with iodobenzene or bromobenzene caused a decrease in the most probable nanoparticle size by about 2.3 nm (Fig. 3c) and 1.7 nm (Fig. 4a), respectively (Table 4). It is clear from the histogram that the size distribution became asymmetric, indicating a higher dispersion of the Pd(0) nanoparticles. In addition, as a result of their reaction with iodobenzene, the outline of Pd(0) nanoparticles became rounder (Fig. 3c), and small (ca. 2 nm) crystallites appeared (shown on the magnified fragment of Fig. 3c), which could be formed by reduction of Pd(II) (like Pd(Ph)(I)) species, the products of oxidative addition of PhI to Pd-PVP. Compared with iodobenzene, the effect of bromobenzene is weaker; however, a shift of the nanoparticle size distribution center toward smaller crystallites and asymmetry of nanoparticle size distribution were also observed (Fig. 4a).

However, the most significant changes in the Pd nanoparticle morphology were observed in the sample of the Pd-PVP colloid warmed with iodobenzene and $[Bu_4N]Br$ (Fig. 3d, Table 4). The center of the size distribution shifted markedly toward smaller particles with a size of ca. 7.6 nm, and large number of small (2–4 nm) particles appeared. It can be seen distinctly that $[Bu_4N]Br$, although itself not reacting

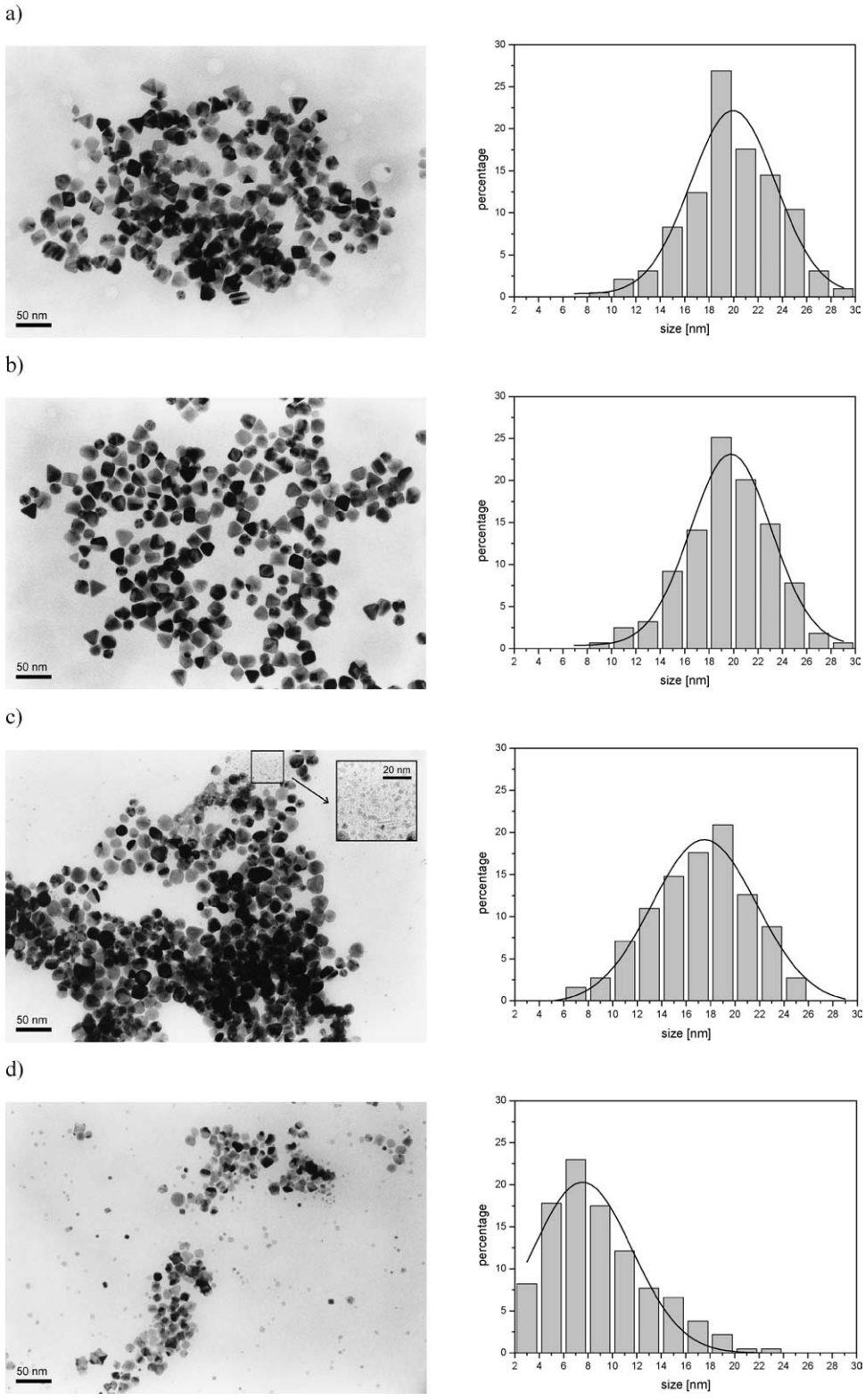

Fig. 3. TEM micrographs and nanoparticles size distributions in the following systems: as prepared Pd-PVP colloid (a), Pd-PVP colloid + $[Bu_4N]Br$ (b), Pd-PVP colloid + PhI (c), Pd-PVP colloid + PhI + $[Bu_4N]Br$ (d).

with palladium nanoparticles, strongly enhanced their interaction with iodobenzene, leading to Pd colloid redispersion. This unexpected effect was also confirmed in reactions of Pd-PVP with bromobenzene and tetrabutyl ammonium salts, $[Bu_4N]X$ (where X = Cl, Br, I). In all cases a Pd nanoparticle size decrease was observed (Table 4), and changes in Pd(0) nanoparticle shape and size distribution were strongly dependent on the kind of halogen anion used.

Table 4
Pd(0) nanoparticle size distribution in Pd-PVP colloid as prepared and after the reactions[a] with PhX (X = Br, I) and/or $[Bu_4N]X$ (X = Cl, Br, I) (Gauss curve approximation)

Sample	Molar ratio	Centre of nanoparticle size distribution (nm)	FWHM (nm)
Pd-PVP	As prepared	19.8	7.0
Pd-PVP + NBu_4Br	1:1	19.8	6.8
Pd-PVP + PhI	1:6	17.5	8.6
Pd-PVP + PhI + $[Bu_4N]Br$	1:6:3	7.6	8.1
Pd-PVP + PhBr (**1**)[b]	1:6	18.1	6.4
Pd-PVP + PhBr + $[Bu_4N]Cl$	1:6:3	17.8	7.3
Pd-PVP + PhBr + $[Bu_4N]Br$ (**2**)[b]	1:6:3	17.3	6.5
Pd-PVP + PhBr + $[Bu_4N]I$	1:6:3	11.7	8.2

[a] Reaction conditions: see experimental part.
[b] Abbreviations of samples used for XPS measurements.

For $[Bu_4N]Cl$ (Fig. 4b), the center of the Pd nanoparticle size distribution shifted slightly toward smaller crystallites, and, moreover, the particles became rounded. Similar but more distinct effects were observed when $[Bu_4N]Br$ was applied (Fig. 4c). The most significant changes in the nanoparticle size distribution were noted when $[Bu_4N]I$ was used (Fig. 4d). The center of size distribution is clearly shifted toward small crystallites (11.7 nm) (Table 4). The width of the nanoparticle size distribution increased, and the shape of palladium particles became more irregular.

3.3. XPS studies of Pd-PVP under Heck reaction conditions

3.3.1. Palladium

The XPS spectrum of as-prepared Pd-PVP showed a signal for Pd $3d_{5/2}$ with a dominating Pd^0 line (BE = 335.1 eV) and an additional Pd^{2+} line (BE = 336.9 eV) (Table 5, Fig. 5). The Pd^{2+} line was first thought to originate from $PdCl_2$ or $PdCl_4^{2-}$, and that assumption appeared to be the most likely, considering the method of Pd-PVP preparation from $PdCl_2$ solution containing HCl and the content of 1–2% chloride ions in the freshly prepared sample (Table 6). However, experimentally found BE values of 337.5 and 337.9 eV for $PdCl_2$ and K_2PdCl_4, respectively, are too different from the 336.9 eV found for the as-prepared Pd-PVP. Therefore, that peak was assigned to PdO, which accompanies Pd^0 left in an oxygen-containing environment [34,35]. This was proved by XPS measurements of Pd-PVP over time, which showed the Pd^0 content to decrease from ca. 82% (in the as-prepared sample) to ca. 25% after 3 months' exposure to the air (Fig. 5).

The XPS-determined palladium content on the surface (before and after reaction with PhI) was ca. 0.2%, that is, much less than the total content volume (5%) (Table 6). This may suggest that the surface of Pd-PVP was covered by a protecting polymer (PVP).

For further studies two samples of Pd-PVP colloid, previously analyzed by TEM, were selected: **1**, Pd-PVP + PhBr; **2**, Pd-PVP + PhBr + $[Bu_4N]Br$; and sample **3**, prepared by heating of a mixture containing Pd-PVP + PhBr + $[Bu_4N]Br$ + $CH_2CHC(O)OBu$ at a component ratio of 1:6:3:6.

Table 5
XPS determined binding energies (BE) (eV)

Sample/BE	Br $3d_{5/2}$ (eV)	N 1*s* (eV)	Pd $3d_{5/2}$ (eV)
PVP		399.0	
$PdCl_2$			337.5
K_2PdCl_4			337.9
Pd^0/Al_2O_3			335.1
PdO/Al_2O_3			336.9
Pd-PVP (as prepared)		399.3	335.1 (82%)
			336.9 (18%)
Pd-PVP + PhBr **(1)**		399.5	336.9
Pd-PVP + PhBr + $[Bu_4N]Br$ **(2)**	66.8 (29%)	402.0	337.0
	68.0 (71%)		
Pd-PVP + PhBr + $[Bu_4N]Br$ + CH_2=CHC(O)OBu **(3)**	66.8 (40%)	402.0	336.8
	68.0 (60%)		
$[Bu_4N]_2[PdBr_4]$	68.0 (100%)		337.1
$[Bu_4N]Br$	66.8 (100%)	401.8	

In all of the samples under study, total oxidation of Pd^0 with PhBr was confirmed. This was indicated by the disappearance of the peak at BE = 335.1 eV (characteristic for Pd^0) and the appearance of a signal at a higher BE value (Table 5, Fig. 6b–d). It is worth noting that reaction of Pd-PVP with only PhBr (sample **1**) led to the oxidation of Pd^0 to Pd^{2+} as a consequence of the oxidative addition reaction

$$Pd^0 + PhBr \rightarrow Br\text{–}Pd(II)\text{–}Ph.$$

This is important because in both Heck and carbonylation reactions the activation of the aryl halide molecule is an essential step in the mechanism [3,36]. Interesting observations resulted from a comparison of the peak half-width (FWHM) of sample **1** (Fig. 6b), 2.3 eV, with those measured for samples **2** and **3**, 1.44 eV and 1.50 eV, respectively (Figs. 6c and d). The BE value for Pd $3d_{5/2}$ of sample **1** was estimated to be 336.89 eV and confirmed the presence of oxidized forms of palladium. The greater half-width of the peak for sample **1** may suggest the presence of different oxidized forms of palladium, for example, some Pd^+ in addition to the main form of Pd^{2+}.

The peaks observed for samples **2** and **3**, both containing PhBr and $[Bu_4N]Br$, have smaller half-width, and the BE values for Pd $3d_{5/2}$ were estimated to be 336.96 and

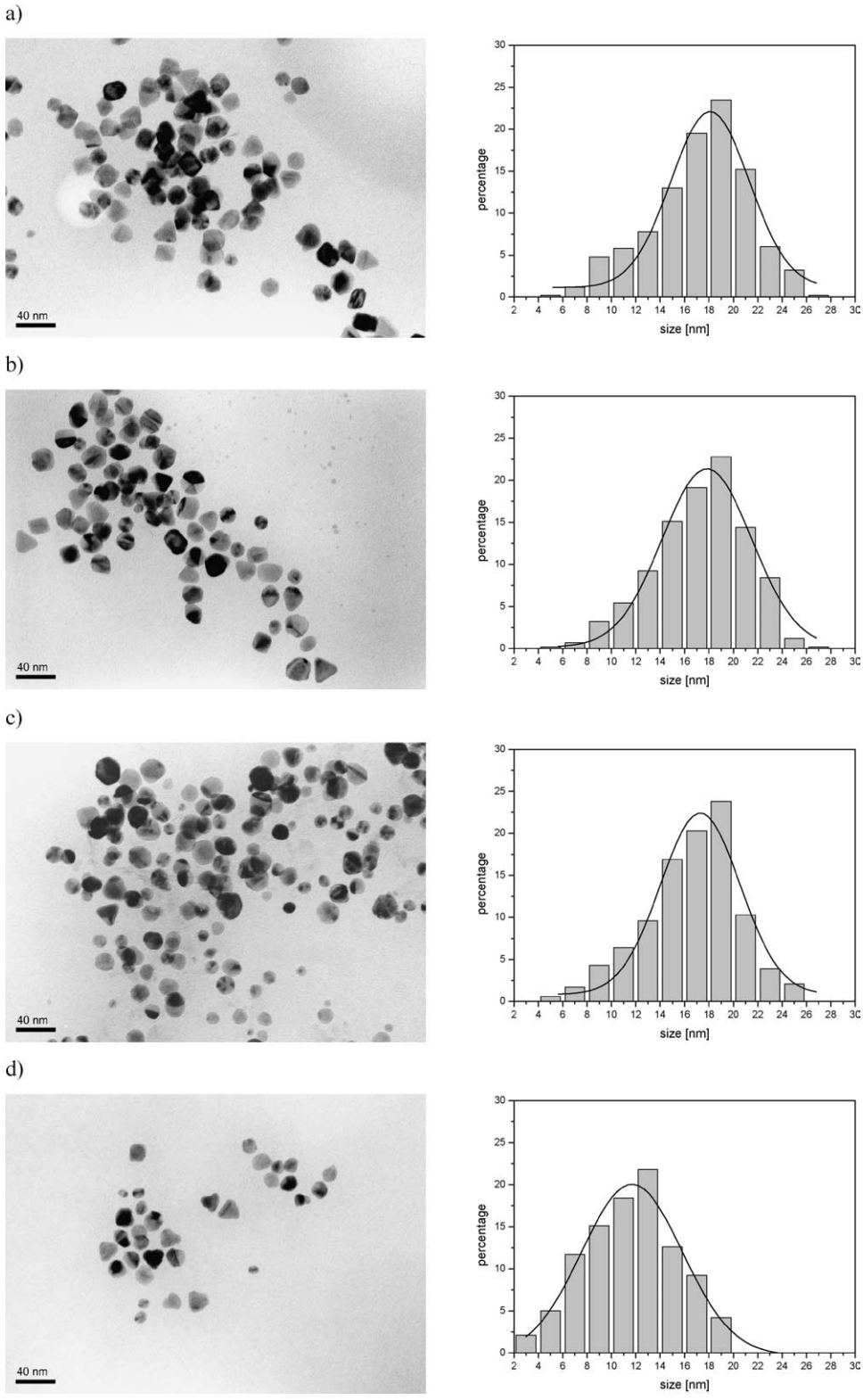

Fig. 4. TEM micrographs and nanoparticles size distributions in the following systems: Pd-PVP colloid + PhBr (a), Pd-PVP colloid + PhBr + $[Bu_4N]Cl$ (b), Pd-PVP colloid + PhBr + $[Bu_4N]Br$ (c), Pd-PVP colloid + PhBr + $[Bu_4N]I$ (d).

336.83 eV, respectively (Table 5). These BE values are very close to that found for $[Bu_4N]_2[PdBr_4]$, which was 337.06 eV. This supports the conclusion that Pd^0 was oxidized via oxidative addition to Pd^{2+}, which was subsequently stabilized mainly as $PdBr_4^{2-}$. Small shift of peaks (in both samples **2** and **3**) toward reduced forms of palladium may indicate the presence of traces of palladium in a lower oxidation state or another form of Pd^{2+} complex, for

Table 6
XPS determined atomic composition (at%)

	PVP	Pd-PVP as prepared	Pd-PVP after 3 months	Pd-PVP + PhBr **(1)**	Pd-PVP + PhBr + $[Bu_4N]Br$ **(2)**	Pd-PVP + PhBr + $[Bu_4N]Br$ + CH_2=CHC(O)–OBu **(3)**
C	75	75.99	71.19	82.82	78.06	68.75
N	10.7	8.83	9.97	9.64	2.48	4.05
O	12.68	14.29	17.25	4.72	13.00	21.68
Si	1.63	0.00		0.00	0.00	0.00
Cl		0.73	1.41	2.63	1.05	1.41
Br		0.00	0.00	0.00	5.06	3.88
Pd		0.16	0.17	0.19	0.35	0.23
Total	100.01	100	99.99	100	100	100

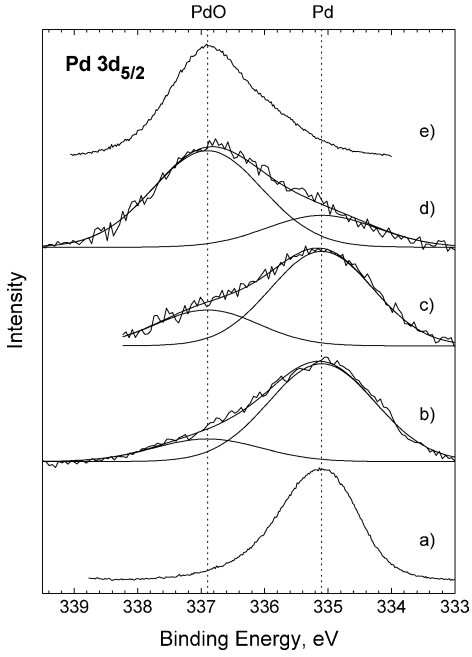

Fig. 5. (a) Pd^0/Al_2O_3, (b) Pd-PVP as prepared, (c) Pd-PVP after 3 days, (d) Pd-PVP after 3 months, (e) PdO/Al_2O_3.

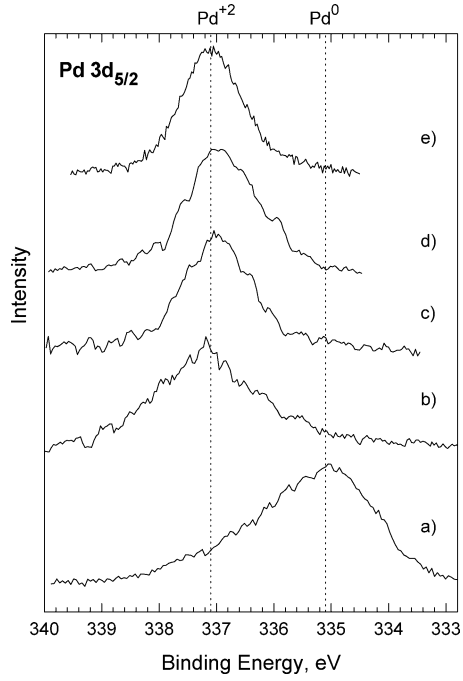

Fig. 6. (a) Pd-PVP as prepared, (b) sample **1**: Pd-PVP + PhBr, (c) sample **2**: Pd-PVP + PhBr + $[Bu_4N]Br$, (d) sample **3**: Pd-PVP + PhBr + $[Bu_4N]Br$ + CH_2=CHC(O)OBu, (e) $[Bu_4N]_2[PdBr_4]$.

example, $[Pd(Ph)_xBr_y]^{2-}$ $(x + y = 4)$, containing a bonded Ph ligand originating from PhBr. The formation of $PdBr_4^{2-}$ was proposed earlier for electrochemically obtained palladium composite in tetraoctylammonium bromide stabilized by polypyrrole [37].

3.3.2. Nitrogen

According to XPS measurements, the BE for N 1s in pure PVP was 399 eV (Fig. 7a), and in the presence of Pd-PVP it was shifted toward slightly higher energy (399.3 eV) (Fig. 7b), which suggested interaction of Pd with polymer nitrogen [38]. In samples **2** and **3**, which additionally contained $[Bu_4N]Br$, a new peak appeared, with a maximum estimated to be 402 eV. The appearance of this peak indicated that the surfaces of both samples (**2** and **3**) were covered with ammonium salt, for which BE for N 1s is 401.75 eV (Fig. 7f). This proposition is additionally supported by the identical shapes of all three curves (Lorentz:Gauss ratio) as well as a FWHM at 1.19 eV.

From the data collected in Table 6 one may conclude that in the samples **2** and **3** the detected amount of nitrogen was much lower than in pure Pd-PVP colloid or in sample **1**. It can be seen from Fig. 7 that in sample **2** practically all of the nitrogen comes from the $[Bu_4N]^+$ cation, whereas only traces of nitrogen originating from PVP were detected on the surface.

A quite different picture was observed for sample **3**, where nitrogen concentration on the surface was twice as high because of the fresh appearance of PVP nitrogen. This is explained as a result of the next step in the Heck reaction, in which the Ph^- ion, coordinated to palladium after oxidative addition of PhBr to Pd-PVP, reacted with butylacrylate and produced butylphenylacrylate. Butylphenylacrylate (or diphenylbutylacrylate) left the surface and uncovered a deeper layer of PVP, causing an increase in the peak of PVP nitrogen.

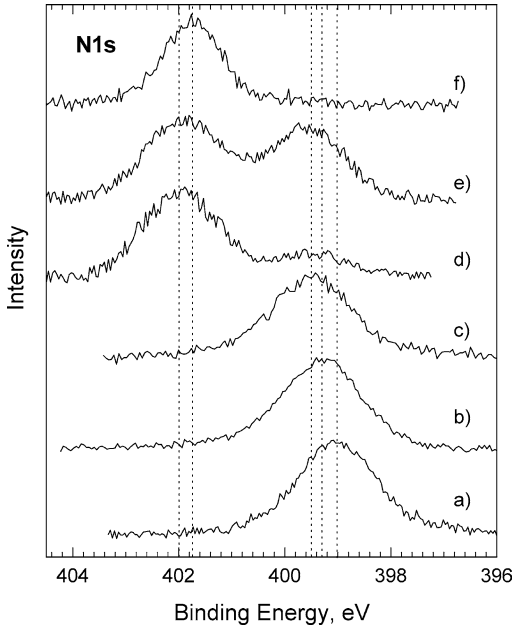

Fig. 7. (a) PVP, (b) Pd-PVP as prepared, (c) sample **1**: Pd-PVP + PhBr, (d) sample **2**: Pd-PVP + PhBr + $[Bu_4N]Br$, (e) sample **3**: Pd-PVP + PhBr + $[Bu_4N]Br$ + CH_2=CHC(O)OBu, (f) $[Bu_4N]Br$. The BE values marked from right to left: 399, 399.3, 399.5, 401.75, and 402 eV.

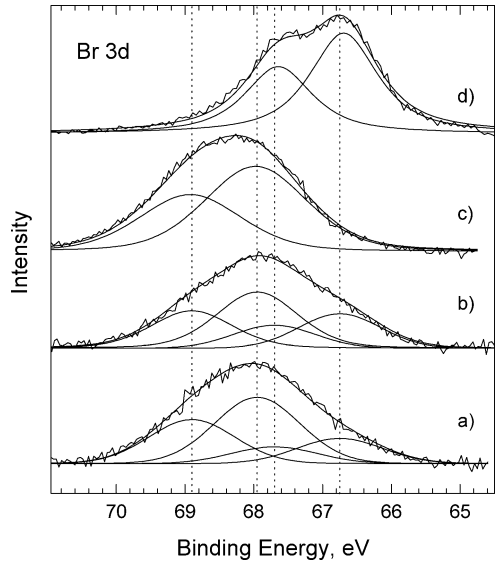

Fig. 8. The Br $3d_{7/2}$ and Br $3d_{5/2}$ deconvoluted spectra of (a) sample **2**: Pd-PVP + PhBr + $[Bu_4N]Br$, (b) sample **3**: Pd-PVP + PhBr + $[Bu_4N]Br$ + CH_2=CHC(O)OBu, (c) $[Bu_4N]_2[PdBr_4]$, (d) $[Bu_4N]Br$.

Further characterization of compounds present in the samples under study was obtained from XPS analysis of bromine, which led to the identification of two compounds, $[Bu_4N]Br$ and $[Bu_4N]_2[PdBr_4]$, on the surface of samples **2** and **3**.

3.3.3. Bromine

From the shape of the Br 3*d* spectrum of samples **2** and **3** one may assume that bromine occurred in at least two different compounds, identified as $[Bu_4N]Br$ and $[Bu_4N]_2[PdBr_4]$ by comparison with model samples (Figs. 8a, b), which is in agreement with earlier analyses of N 1*s* and Pd 3*d* XPS data. Binding energies (BE) of Br $3d_{5/2}$ and Br $3d_{3/2}$ for $[Bu_4N]Br$ were estimated to be 66.75 and 67.7 eV, whereas for $[Bu_4N]_2[PdBr_4]$ they were estimated at 67.95 and 68.9 eV, respectively. From the quantitative analysis of samples **2** and **3** one can conclude that the relative contribution of $[Bu_4N]_2[PdBr_4]$ in sample **3** decreased from ca. 70 to 60% in comparison with sample **2**. This may suggest partial dissolution of $[Bu_4N]_2[PdBr_4]$ and its elimination from the surface or the appearance of another compound covering the surface.

Reaction of Pd-PVP colloid with aryl halides (PhBr or PhI) caused Pd^0 oxidation and formation of Ph-Pd(II)-X fragments; however, their concentration on the surface was rather low. At such a concentration of palladium, bromide ions bonded to Pd^{2+} were not detected, because of the ca. 5 times lower sensitivity of the spectrometer for Br compared with that for Pd (atomic sensitivity factors for Pd = 4.642 and for Br = 0.895).

However, reaction of Pd-PVP colloid with PhBr in the presence of $[Bu_4N]Br$ leads to the formation of $[Pd(Ph)Br_3]^{2-}$ and $[PdBr_4]^{2-}$ anions containing a higher content of bromides per palladium atom, and as a consequence the concentration of bromine atoms on the surface increased (Table 6). Simultaneously, the spectrum of nitrogen from the $[Bu_4N]^+$ cation became visible, whereas the spectrum of PVP nitrogen was practically undetected. After reaction with *n*-buthylacrylate, the Heck reaction products (arylated olefine and palladium-containing species) were removed from the surface, leading to a decrease in palladium and bromine contents.

3.4. UV–vis spectra

UV–vis spectra of samples **2** and **3** were measured in methanol in the range of 300–600 nm. No bands were observed for either sample, or for Pd-PVP colloid warmed with PhBr or PhI. However, when Pd-PVP was warmed with PhI in the presence of $[Bu_4N]Br$ or $[Bu_4N]I$ (reaction conditions are given in the Table 4), new bands appeared at 418 and 444 nm, respectively. The absorption band at 418 nm observed for the reaction product of Pd-PVP + PhI + $[Bu_4N]Br$ lies close to that found at 408 nm for $[Bu_4N]_2[PdBr_4]$, and this observation supported the interpretation of the XPS data. The UV–vis spectrum of the product obtained in the reaction of Pd-PVP + PhI + $[Bu_4N]I$, with a maximum at 444 nm, was similar to that reported by Reetz, who observed a band at 450 nm [12]. The different positions of the UV–vis bands in these two samples reflected the influence of the kind of halogen ion in $[PdX_4]^{2-}$ ions.

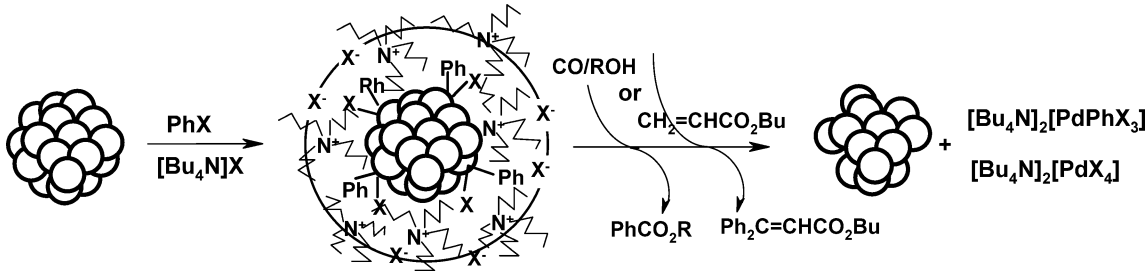

Scheme 3.

4. Summary

- Pd-PVP colloid (19.8-nm diameter) in $[Bu_4N]Br$ medium is catalytically active in Heck coupling of bromobenzene with butyl acrylate and methoxycarbonylation of iodobenzene.
- By two independent methods, TEM and XPS, it was found that Pd-PVP colloid reacted with aryl halides (PhX, X = Br, I) to form Pd(II) complexes containing a X-Pd(II)-Ph fragment as a result of oxidative addition. This reaction caused a small decrease in Pd nanoparticle size, from 19.8 to 17.5 nm.
- The same reaction of Pd-PVP colloid carried out in the presence of $[Bu_4N]Br$ led to the formation of soluble $[Bu_4N]_2[Pd(Ph)Br_3]$- or $[Bu_4N]_2[PdBr_4]$-type complexes, which then most probably participated in a catalytic reaction in the solution. The formation of these products was additionally proved by UV–vis spectroscopy.
- TEM measurements of the Pd-PVP colloid after the reaction with PhX and $[Bu_4N]X$ showed a significant reduction in the Pd nanoparticle size as a result of palladium oxidation and solubilization. To our knowledge this is the first reported evidence of Pd nanoparticle redispersion during a reaction.

The results of previously published papers did indicate some agglomeration of nanoparticles during catalytic reaction and the formation of bigger crystallites. In our studies, which are related to the Heck reaction and to carbonylation reaction conditions, the Pd(0) nanoparticle size decrease was observed when Pd-PVP colloid was heated with PhX + $[Bu_4N]X$ (X = Br, I), and most probably the same phenomenon will happen with any other aryl halide and ammonium salt.

The results obtained make it possible to postulate an important contribution of soluble palladium complexes in reactions catalyzed by Pd-PVP colloid and an essential role for ammonium salts in palladium transfer from the colloidal form to soluble monomolecular complexes (Scheme 3).

The problem of equilibrium between colloidal Pd form and soluble Pd monomolecular forms was discussed for carbonylation [39], hydrogenation in water-in-oil-microemulsion [40], and the Heck reaction [41]. In all of the above-mentioned cases, the formation of soluble palladium compounds was proposed or experimentally proved. On the other hand, however, palladium leaching from the Pd/C catalyst used for the Heck reaction in ionic liquids was not found [42].

- The appearance of new, very small crystallites in Pd-PVP colloid samples after reaction with PhX + $[Bu_4N]X$ (Fig. 3d) may be explained by the reduction of Pd(II) complexes of the $[Pd(Ph)X_3]^{2-}$ or $[PdX_4]^{2-}$ type. Methanol, always present as a solvent, could serve as a reducing agent for Pd(II).
- Our studies clearly show that Pd-PVP colloid is a precursor of soluble forms of the catalyst, which subsequently are again reduced to colloidal forms of lower size.

Acknowledgments

Financial support by the State Committee for Scientific Research KBN (Poland) (Grant 3T09A 115 26) is gratefully acknowledged. The authors are indebted to Jean-Charles Wypych at Clermont-Ferrand and Dr. Ewa Mieczyńska for technical assistance.

References

[1] B. Cornils, W.A. Herrmann (Eds.), Applied Homogeneous Catalysis with Organometallic Compounds, in: A Comprehensive Handbook in Two Volumes, VCH, Weinheim–New York, 1996.
[2] R. Skoda-Foldes, L. Kollar, Current Organic Chem. 6 (2002) 1097.
[3] I.P. Beletskaya, A.V. Cheprakov, Chem. Rev. 100 (2000) 3009.
[4] S.J. Danishefsky, J.J. Masters, W.B. Young, J.T. Link, L.B. Snyder, T.V. Magee, D.K. Jung, R.C.A. Isaacs, W.G. Bornmann, C.A. Alaimo, C.A. Coburn, M.J. Di Grandi, J. Am. Chem. Soc. 118 (1996) 2843.
[5] S.C. Stinson, Chem. Eng. News (1999) 81.
[6] N. Miyaura, A. Suzuki, Chem. Rev. 95 (1995) 2457.
[7] H. Remmele, A. Kollhofer, H. Plenio, Organometalics 22 (2003) 4098.
[8] C. Amatore, A. Jutand, Acc. Chem. Res. 33 (2000) 314.
[9] Q. Yao, E.P. Kinney, Z. Yang, J. Am. Chem. Soc. 68 (2003) 7528.
[10] A.F. Schmidt, V.V. Smirnov, J. Mol. Catal. A Chem. 203 (2003) 75.
[11] C. Gurtler, S.L. Buchwald, Chem. Eur. J. 5 (11) (1999) 3107.
[12] M.T. Reetz, E. Westermann, Angew. Chem., Int. Ed. 39 (1) (2000) 165.
[13] R.R. Deshmulch, R. Rajagopal, K.V. Srinivasan, Chem. Commun. (2001) 1544.
[14] A.M. Trzeciak, W. Wojtków, J.J. Ziółkowski, J. Wrzyszcz, M. Zawadzki, New J. Chem. 28 (2004) 859.
[15] J.D. Aiken III, R.G. Finke, J. Mol. Catal. A Chem. 145 (1999) 1.

[16] M. Beller, H. Fischer, K. Kuhlein, C.-P. Reisinger, W.A. Herrmann, J. Organomet. Chem. 520 (1996) 257.
[17] L.A. Fowley, D. Michos, X.-L. Luo, R.H. Crabtree, Tetrahedron Lett. 34 (19) (1993) 3075.
[18] M.T. Reetz, J.G. De Vries, Chem. Commun. 14 (2004) 1559.
[19] T. Jeffery, Tetrahedron Lett. 35 (19) (1994) 3051.
[20] T. Jeffery, J.-C. Galland, Tetrahedron Lett. 45 (24) (1994) 4103.
[21] T. Jeffery, M. David, Tetrahedron Lett. 39 (1998) 5751.
[22] V. Calo, A. Nacci, L. Lopez, A. Napola, Tetrahedron Lett. 42 (2001) 4701.
[23] V. Calo, A. Nacci, A. Monopoli, A. Detomaso, P. Iliade, Organometalics 22 (2003) 4193.
[24] V. Calo, A. Nacci, L. Lopez, N. Mannarini, Tetrahedron Lett. 41 (2000) 8973.
[25] M.T. Reetz, R. Breinbauer, K. Wanninger, Tetrahedron Lett. 37 (26) (1996) 4499.
[26] G. Zou, Z. Wang, J. Zhu, J. Tang, M.Y. He, J. Mol. Catal A Chem. 206 (2003) 193.
[27] V. Calo, A. Nacci, A. Monopoli, S. Laera, N. Cioffi, J. Org. Chem. 68 (2003) 2929.
[28] H. Bonnemann, R. Brinkmann, R. Koppler, P. Neiteler, J. Richter, Adv. Mater. 4 (1992) 804.
[29] S. Klingelhofer, W. Heitz, A. Greiner, S. Oestreich, S. Forster, M. Antonietti, J. Am. Chem. Soc. 119 (1997) 10116.
[30] D.D. Perrin, W.L.F. Armarego, D.R. Perrin, Purification of Laboratory Chemicals, Pergamon, Oxford, 1986.
[31] H.P. Choo, K.Y. Liew, H. Liu, J. Mater. Chem. 12 (2002) 934.
[32] H.P. Choo, K.Y. Liew, W.A.K. Mohamood, H. Liu, J. Mater. Chem. 11 (2001) 2906.
[33] J.J. Ziółkowski, A. Gniewek, W. Tylus, in: 14th Internat. Symposium on Homogeneous Catalysis, Munich, Germany, 5–9 May, 2004, poster 0040.
[34] E.H. Voogt, A.J.M. Mens, O.L.J. Gijzeman, J.W. Gens, Surf. Sci. 350 (1996) 21.
[35] G.R. Cairns, R.J. Cross, D. Stirking, J. Mol. Catal. A Chem. 172 (2001) 207.
[36] J.-L. Malleron, J.-C. Fiand, J.-Y. Legros, Handbook of Palladium – Catalyzed Organic Reactions. Synthetic Aspects and Catalytic Cycles, Academic Press, 1997.
[37] N. Cioffi, L. Torsi, I. Losito, L. Sabbatini, P.G. Zambonin, T. Bleve-Zacheo, Electrochim. Acta 46 (2001) 4205.
[38] D. Atzei, D. De Filippo, A. Rossi, M. Porcelli, Spectr. Acta A 57 (2001) 1073.
[39] F. Bertoux, E. Monflier, Y. Castanet, A. Mortreux, J. Mol. Catal. A Chem. 143 (1999) 23.
[40] B. Yoon, H. Kim, C.M. Wai, Chem. Commun. (2003) 1041.
[41] A. Biffis, M. Zecca, M. Basato, Eur. J. Inorg. Chem. (2001) 1131.
[42] H. Hagiwara, Y. Shimizu, T. Hoshi, T. Suzuki, M. Ando, K. Okhubo, C. Yokoyama, Tetrahedron Lett. 42 (2001) 4349.